Journal of *Marine Science and Engineering*

MDPI

*Article*

# Performance of Network Real-Time Kinematic in Hydrographic Surveying

**Mohamed Elsayed Elsobeiey**

Department of Hydrographic Surveying, Faculty of Maritime Studies, King Abdulaziz University, Jeddah 21589, Saudi Arabia; melsobeiey@kau.edu.sa

**Abstract:** The main objective of this paper is to investigate the performance of the Network Real-time Kinematic (NRTK) technique in hydrographic surveying and check whether it meets the International Hydrography Organization (IHO) minimum bathymetry standards for the safety of navigation hydrographic surveys. To this end, the KAU-Hydrography 2 vessel was used to conduct a hydrographic survey session at Sharm Obhur. NRTK corrections were streamed in real time from the KSA-CORS NTRIP server and GNSS data were collected at the same time at the base station using a Trimble SPS855 GNSS receiver. Multibeam records were collected using a Teledyne RESON SeaBat T50-P multibeam echosounder in addition to Valeport's sound velocity profiler records and Applanix POSMV data. Applanix POSPac MMS 8.3 software was used to process the GNSS data of the base station along with the POSMV data to obtain the Smoothed Best Estimate of Trajectory (SBET) file, which is used as a reference solution. The NRTK solution is then compared with the reference solution. It is shown that the Total Horizontal Uncertainty (THU) and the Total Vertical Uncertainty (TVU) of the NRTK solution are 6.38 cm and 3.10 cm, respectively. Statistical analysis of the differences between the seabed surface generated using the NRTK solution and the seabed surface generated using the Post-Processed Kinematic (PPK) technique showed an average of −0.19 cm and a standard deviation of 2.4 cm. From these results, we can conclude that the KSA-CORS NRTK solution successfully meets IHO minimum bathymetry standards for the safety of navigation hydrographic surveys at a 95% confidence level for all orders of hydrographic surveys.

**Keywords:** hydrographic surveying; bathymetry; NRTK; IHO



Academic Editors: Salvatore Gaglione and Franc Dimc

Received: 23 November 2024
Revised: 29 December 2024
Accepted: 30 December 2024
Published: 1 January 2025

**Citation:** Elsobeiey, M.E. Performance of Network Real-Time Kinematic in Hydrographic Surveying. *J. Mar. Sci. Eng.* **2025**, *13*, 61. https://doi.org/10.3390/jmse13010061



## 1. Introduction

Typically, real-time kinematic (RTK) GNSS positioning has been used for high-accuracy positioning applications. The high accuracy of this method comes from the fact that both base and rover GNSS receivers are close enough to share a high degree of similarity of errors and biases. The shorter the receiver's separation, the closer the errors and biases are. As a result, most GNSS errors and biases are removed by differencing, leading to centimeter-level positioning accuracy and fixing of carrier phase ambiguity parameters [1]. However, the accuracy of the RTK positioning method is limited by the base-rover separation, which is about 15 km [2]. Beyond this distance, the errors at both base and rover GNSS receivers (mainly ionospheric and tropospheric delays) are less correlated, i.e., they would not cancel out sufficiently through differencing. As a result, it will be difficult to fix the carrier phase ambiguity, causing the positioning accuracy to deteriorate [3,4].

To overcome the base–rover distance limitation, the multi-base positioning technique was investigated by several researchers. Such a technique is well-known as network RTK

(NRTK). Vollath et al. [5] introduced multi-base RTK positioning using a virtual reference station (VRS) that is close to the rover position. As a result, errors at both base and rover receivers are effectively canceled out by differencing. Their results showed reliability and accuracy improvement in addition to better ambiguity resolution compared with the classical RTK method. The bilinear interpolation technique was used to interpolate the errors at the rover location using a permanent network of base stations [6]. He showed promising results for using multi-base stations, especially for ambiguity fixing rates over the traditional RTK method. Landau et al. [7] investigated the performance of VRS and Flaechen Korrektur Parameter (FKP) methods. They showed that the FKP method has some limitations in ionospheric residual interpolation at the rover position since the rover does not send its own location to the control center; in addition, the validity of corrections in this method depends on the base–rover distance. However, these disadvantages did not exist in the VRS technique, since the rover continuously updates and sends its position to the control center. It is possible to obtain precise mobile mapping for a 40 km trajectory using NRTK [8]. Aponte et al. [9] examined the United Kingdom CORS for NRTK applications. They showed that the results of all static tests using NRTK observations generated from the UK-CORS are more accurate and precise than the conventional short- and long-baseline RTK solutions. Dardanelli et al. [10] examined the VRS, FKP, and nearest station NRTK techniques for static positioning. They showed that the VRS NRTK technique is superior to the other two methods, achieving centimeter and decimeter accuracies in horizontal and vertical coordinates components, respectively. Centimeter and 5–7 cm accuracy levels can be achieved in horizontal and vertical coordinates components using VRS generated from the Malaysia NRTK, respectively [11]. Cina et al. [3] investigated VRS NRTK using regional (inter-station distance of about 40–50 km) and national (inter-station distance of about 80–100 km) GNSS networks. They showed that 1.5 cm and 1.8 cm can be achieved for 2D and 3D coordinates' standard deviation using VRS NRTK from the regional network compared with 3.1 cm and 4.1 cm 2D and 3D coordinates' standard deviation using VRS NRTK from the national network. Andrzej et al. [12] tested whether integration of differential GPS and inertial navigation systems (DGPS/INS) meets the accuracy requirements of IHO different survey orders. They found that the RTK system meets the accuracy requirements of all IHO survey orders, and they proved that the DGPS system does not meet the accuracy requirements of the exclusive order.

Multistate reliability theory was applied to improve NRTK's results by identifying the NRTK's system critical components to make the system more robust [13]. Ouassou and Jensen [14] introduced NRTK data integrity to improve the rover position in the field by means of NRTK data screening using multivariate statistical analysis. El-Diasty [15] showed that sub-decimeter kinematic positioning accuracy can be achieved using NRTK from Saudi Arabia CORS. Zhang et al. [16] improved the initialization speed for long-range NRTK using network processing mode rather than baseline mode to fix the network carrier-phase ambiguities. They showed that the estimated float ambiguity is more consistent and accurate, which improved the initialization speed by 18%. Gökdaş and Özlüdemir [17] developed an experimental variance model to account for the NRTK baseline length effect on the position accuracy. They used VRS and FKP methods at different baseline lengths. They found that there is no significant correlation with positional accuracy for baselines up to 40 km. However, they developed a variance model as they found a linear correlation of 69.2% with precision. They found that better results can be obtained using the variance model than the linear model. de Andrade Neto et al. [18] investigated the effect of satellite-based correction service on the vertical component accuracy to obtaining sensor position during multibeam bathymetric survey. They estimated the depth surface using both the MarineStar correction service and the post-processed kinematic (PPK) technique. They

concluded that the PPK-based depth surface met the hydrographic standards, while the MarineStar products did not. Santana et al. [19] compared the data obtained from a tide gauge with PPP and PPK methods. They showed that PPK was able to fulfill the requirements for the IHO-exclusive order in 100% of six periods of survey when the vessel was moored, using the Tide Gauge as a reference. For the PPP, this value was 50% having the PPK as a reference for 12 periods, with the vessel moored or sailing.

Precise point positioning (PPP), on the other hand, offers a distinct advantage over differential methods. However, PPP requires mitigation of all error sources that are usually canceled out in differential methods. The main challenge of PPP, however, is the convergence time. The PPP solution requires more than 20 min convergence time if dual-frequency data are used [20]. Extensive research is underway to reduce the PPP solution convergence time using triple-frequency combination, multi-system integration, supplementary corrections, and more complicated algorithms. Elsobeiey and El-Rabbany [21] showed that the convergence time can be reduced by about 10% using triple-frequency measurements (L1, L2 and L5). Modeling observable-specific phase bias (phase OSBs) has a great effect on PPP ambiguity resolution (PPP-AR) and hence improves the convergence time. Geng et al. [22] developed an approach to estimate the phase OSBs of all dual-frequency combinations (L1/L2 and L1/L5 for GPS and E1/E5a, E1/E5b, E1/E5, and E1/E6 for Galileo). They showed that 95% ambiguity fixing rates can be achieved for both wide-lane and narrow-lane ambiguities and 30–60% position precision improvement in the east component in all tested dual-frequency PPP combinations. PPP-AR and convergence time reduction can be achieved using the undifferenced decoupled clock model [23]. Elsobeiey and El-Rabbany [24] developed a between-satellite single-difference (BSSD) model and used decoupled clock correction to account for code and phase satellite clock errors. They showed that PPP convergence time can be reduced by up to 50% and solution precision can be improved by more than 60% compared with the traditional PPP model.

PPP solution and convergence time can be improved using multi-GNSS constellations. Hou and Zhou [25] showed that a dual-system combination based on Galileo, combined with GPS and the BeiDou navigation satellite system (BDS-3), can improve the RMS and convergence time by 50% compared with the single system. Moreover, dual-systems based on BDS-3 combined with GPS and Galileo can improve the RMS and convergence time by 50% and 60%, respectively, compared with the single system. Zheng et al. [26] showed that GPS has the best performance at low latitudes compared with GLONASS, which is better at high latitudes. However, PPP processing with combined GPS/GLONASS observations reduces the convergence time and improves the accuracy of the tropospheric estimates compared with a single system. Availability of the international GNSS service (IGS) real-time service (RTS), which provides real-time augmentation information, including real-time satellite orbit and clock corrections, showed great potential for real-time PPP with better accuracy and less convergence time [27–29].

The GNSS performance, however, is severely affected by signal interference, especially in areas with limited access to satellite signals such as forests, tunnels, or urban areas. Therefore, it is essential to integrate GNSS with other systems such as an inertial navigation system (INS), ultra-wide band (UWB), and laser imaging, detection, and ranging (LiDAR). Specht [30] tested the navigation parameters (position and orientation) of the GNSS/INS system for unmanned surface vehicles (USVs). He showed that the USV path localization using the GNSS/INS system working in the RTK mode meets the IHO positioning requirements for inland hydrographic surveys even when loss of RTK corrections occurs for an extended period. Huang et al. [31] introduced tightly integrated multi-GNSS PPP with UWB technology. They showed that multi-GNSS/UWB integration can significantly improve positioning performance in terms of positioning accuracy and convergence time.

Li et al. [32] proposed a tightly coupled PPP/ INS/vision/LiDAR integration method to achieve high-precision, continuous, and reliable navigation in urban environments. They showed that PPP/INS/vision/LiDAR integration can maintain sub-meter level positioning in both GNSS half-open-sky and difficult environments, with improvements of 50.7%, 58.6%, and 54.3% and 46.2%, 55.0%, and 58.8% relative to PPP/INS/vision and PPP/INS/LiDAR, respectively. Moreover, they showed that both visual and LiDAR information can significantly improve velocity and attitude estimation performance, especially for the heading. Table 1 summarizes the main strengths and limitations of PPP, RTK, NRTK, and integrated systems.

**Table 1.** Main strengths and limitations of PPP, RTK, NRTK, and integrated systems.

| Technique | Strengths | Limitations |
| --- | --- | --- |
| PPP | • Only single receiver is utilized<br>• Lowest operational cost<br>• Does not require regional network or control center | • Long convergence time<br>• Not applicable for real-time applications except by applying external corrections (may be free of charge such as IGS-RTS corrections or by subscription like Trimble RTX). However, this requires internet connection. |
| RTK | • Provides real-time solution<br>• At least one base station is required rather than a network of reference station<br>• No need for control center | • Requires a robust communication link<br>• Technical problems, or being outside of the cellular (or Internet) coverage over study area, may cause loss of communication/signal<br>• Base–rover separation distance is considered a limitation (within 15 km) |
| NRTK | • Provides real-time solution<br>• Extended coverage up to 70 km from the nearest base station<br>• Considered cheap if CORS is already established and available to use free of charge | • User needs internet connection<br>• Requires extensive infrastructure like network of reference station and control center<br>• The distribution and density of the network stations, cellular network coverage, and environmental dynamics have significant impacts on the obtainable precision |
| GNSS/INS integrated System | • Provides real-time solution<br>• Provides a more accurate and reliable position<br>• The impact of interference and time delays can be significantly reduced by integration process<br>• The tight coupling scheme improves the quality of navigation solutions<br>• Can be used to add other sensors such as Vision or LiDAR | • Specific care should be considered such as measurement synchronization, level-arm compensation, and GNSS measurement quality control<br>• Platform dynamics influence the choice of inertial sensors as well as navigation algorithms<br>• When adding a new sensor the integration filter is expanded to include new measurement observables and new states (if necessary) without modifying previously developed filter components<br>• Adding a new sensor may influence the choice of the inertial measurement unit |

This paper investigates the performance of NRTK in hydrographic surveying. Analysis of the NRTK positioning technique is compared with the traditional RTK positioning

technique. Moreover, NRTK positioning results are investigated as to whether they meet the minimum standards of the International Hydrography Organization (IHO) for hydrographic surveys.

## 2. NRTK System Description

The NRTK system consists of three main parts. The first part consists of the network of continuous operational reference stations (CORSs), with accurately known positions and well-prepared to transmit their data in real time to the control center. The second part is the control center that collects and analyses data from all stations in real time, performing ambiguity resolution for all satellites of each station, as well as computing ionospheric and tropospheric delays and clock biases. The third part represents the products that are available for users from the control center using specific protocols and formats. Generally, the correction data and metadata are generated in "Radio Technical Commission for Maritime Service" (RTCM) and "Compact Measurement Record" (CMR) formats [17]. Unlike RTK, in which corrections are transmitted to the rover by means of radio modems, NRTK users usually access correction data streams via the Internet using the "Networked Transport of RTCM via an Internet Protocol" (NTRIP) caster [33]. The raw measurements for each station can be stored for post-processing purposes as well.

### 2.1. NRTK Corrections Generation

The mathematical model of code and carrier-phase measurements recorded at one of the permanent stations ($B$) at a specific time ($t$) from satellite ($i$) can be written as follows [24,34]:

$$P_B^i(t) = \rho_B^i(t) + c\Big(dt_B(t) - dt^i(t)\Big) + T_B^i(t) + I_B^i(t) + E_B^i(t) \tag{1}$$

$$\Phi_B^i(t) = \rho_B^i(t) + c\Big(dt_B(t) - dt^i(t)\Big) + T_B^i(t) - I_B^i(t) + \lambda N_B^i + E_B^i(t) \tag{2}$$

where $P_B^i, \Phi_B^i$ are the pseudo range and carrier-phase (scaled to distance (m)) measurements at station $B$ from satellite $i$, respectively; $dt_B, dt^i$ are the receiver and satellite clock errors, respectively; $\lambda$ is the carrier-phase wavelength; $N$ is the carrier-phase ambiguity parameter; $c$ is the speed of light in vacuum (m/sec); $\rho$ is the true geometric distance between satellite antenna phase center and receiver antenna phase center at reception time (m); $I, T$ are the slant ionospheric and tropospheric delays, respectively; and $E$ is the ephemerids error.

Since the accurate coordinates of all CORS are known, the geometric distance can be computed using the known satellite coordinates $\rho_B^i(t) = \sqrt{\left(X_B - X^i(t)\right)^2 + \left(Y_B - Y^i(t)\right)^2 + \left(Z_B - Z^i(t)\right)^2}$. In addition, from the network processing, all carrier-phase ambiguities and clock biases are solved and considered known. All known terms can be moved to the left side of Equations (1) and (2), leading to the so-called pseudorange and carrier-phase differential corrections, respectively, as follows:

$$PRC_B^i(t) = T_B^i(t) + I_B^i(t) + E_B^i(t) \tag{3}$$

$$CPC_B^i(t) = T_B^i(t) - I_B^i(t) + E_B^i(t) \tag{4}$$

where $PRC_B^i$, $CPC_B^i$ are the pseudorange and carrier-phase corrections at reference station ($B$) for specific satellite ($i$), respectively. It is very essential for the control center to make a separation of the ionospheric and tropospheric errors. In general, error sources can be classified into two components, dispersive and non-dispersive. The dispersive component represents the ionospheric delay and the non-dispersive component represents both tropospheric delay and orbital error. If the IGS-precise ephemerides are used to account for

GNSS satellite orbits, the non-dispersive component will include the tropospheric delay only. Once ionospheric and tropospheric delays are determined at all CORS networks, a model of change of such errors can be developed to interpolate at the rover location. The rover receiver, on the other hand, must estimate its own clock error and carrier-phase ambiguities. Based on the NRTK correction forms and the role and computational load of both the control center and the rover receiver, NRTK positioning techniques can be classified into three main types: Virtual Reference Station (VRS), Multi-Reference Station (MRS), and Master Auxiliary Concept (MAC).

#### 2.1.1. Virtual Reference Station (VRS)

In this approach, the rover receiver must send its own location to the control center. Hence, the control center searches the CORS network for at least three stations close to the rover and generates the differential corrections. Then, the control center interpolates and generates a set of corrections at a virtual location, typically at the rover location. In this case, communication between the rover and the control center must be bi-directional so that the rover is able to send its own location continuously to the control center. Once the rover receiver gets the real-time corrections, it starts with fixing ambiguities and hence the computing position.

#### 2.1.2. Multi Reference Station (MRS)

In the MRS method, a local correction model is generated at each reference station of the CORS network. The corrections generated at the closest reference station are broadcasted as a local model in the form of a polynomial function. The polynomial coefficients are referred to as "area parameters", and they are transmitted in both their dispersive (ionospheric bias) and non-dispersive (ephemerids and tropospheric bias) components via the FKP format. Unlike the RTCM, the FKP format is not standard. A decoder software is required at the rover receiver to decrypt the received model and compute the dispersive and non-dispersive correction components.

#### 2.1.3. Master Auxiliary Concept (MAC or MAX)

In this technique, the control center processes GNSS data received from all CORS networks and reduces carrier-phase measurements to a common ambiguity level [35]. A sub-network is then selected to generate the rover corrections. In the case of two-way communications, the sub-network may be predefined or automatically selected by the control center from the network based on the rover location. In the case of broadcast communications, however, such a set of reference stations can be pre-defined by the control center based on the corresponding ambiguity-fixing success rate for each station. The master auxiliary correction differences are generated using the carrier-phase measurements of the selected reference stations corrected by the estimated ambiguities in addition to the common part of the receiver clock and known quantities such as geometric range and satellite clock [36].

To decrease the correction data size, full correction and coordinate information is only supplied for the master station. Correction and coordinate discrepancies are communicated to all other auxiliary stations. Splitting the corrections into dispersive and nondispersive components decreases the required transmission bandwidth since tropospheric and orbital errors are known to vary slowly over time; therefore, the data rate does not need to be as fast as for the dispersive correction [37]. The master station is used for data transmission and has no special role in correction computations. Hence, if data from the master station become invalid or unavailable for whatever reason, one of the auxiliary stations can simply take the function of the master station [38].

The user, on the other hand, can use three different types of products based on the sub-network selection criterion. The first is the pre-defined sub-network, where the subnetworks are pre-defined by the control center based on the rover position. The second is the auto MAX service, in which the sub-network is automatically created based on the rover position. The third is the individual master auxiliary (iMAX), which is similar to the VRS method, where the control center estimates the corrections at the rover position and the rover directly applies such corrections to its own data. Once the rover receives data and corrections from the master station (in the case of the first two products), it can compute the effect of the ionosphere, troposphere, and orbit at its location. Using the ionosphere-free linear combination, the combined influence of the troposphere and orbit can be estimated for each satellite and reference station and then interpolated for the rover's position. Similarly, using the geometry-free linear combination, the ionosphere's impact may be computed for each satellite and reference station and then interpolated for the rover's position. Rover then applies the computed corrections and solves carrier-phase ambiguities and its own position [36]. Figure 1 shows different NRTK techniques and Table 2 summarizes the main differences between such techniques.

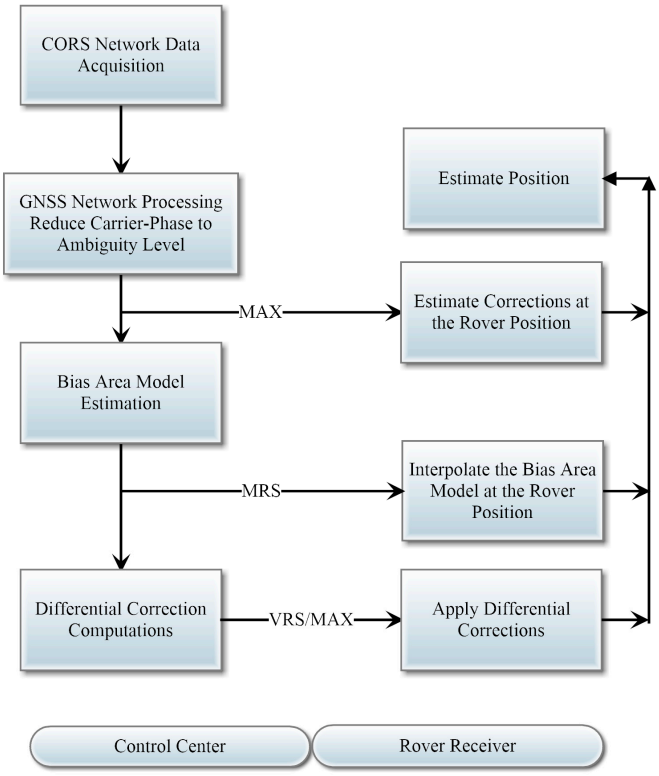


**Figure 1.** Different NRTK techniques.

**Table 2.** Summary of NRTK positioning techniques.

| | VRS | MRS | MAC |
|---|---|---|---|
| Communication type | Two-way | One-way or two-way | Two-way |
| Type of protocols | RTCM 3.x<br>RTCM 2.x messages type 18 & 19 or 20 & 21 | RTCM type 59<br>FKP | RTCM 3.x |
| Control center computational load | Very high | low | low |
| Rover computational load | Very low | Very high | Very high |

### 2.2. KSA-CORS Network

KSA-CORS includes more than 200 continuously operating GNSS reference stations, Figure 2. The network is established and maintained by the General Authority for Survey and Geospatial Information (GASGI) [39]. The KSA-CORS network's goal is to offer a dependable and accurate GNSS positioning service across the Kingdom. Furthermore, it aims to build, disseminate, and maintain the Saudi Arabia National Spatial Reference System (SANSRS), which is known as KSA-GRF17. KSA-GRF17 is defined in such a way that it coincides with the International Terrestrial Reference Frame 2014 (ITRF14) at epoch 2017.0 and co-moves with the stable part of the Arabian tectonic plate [40,41]. KSA-CORS provides subscribed users with different types of real-time positioning services such as NRTK positioning service, differential GNSS (DGNSS) positioning service, and single-station RTK positioning service. In addition to real-time positioning service, subscribed users can download raw GNSS data and VRS GNSS data at known locations for post-processing.

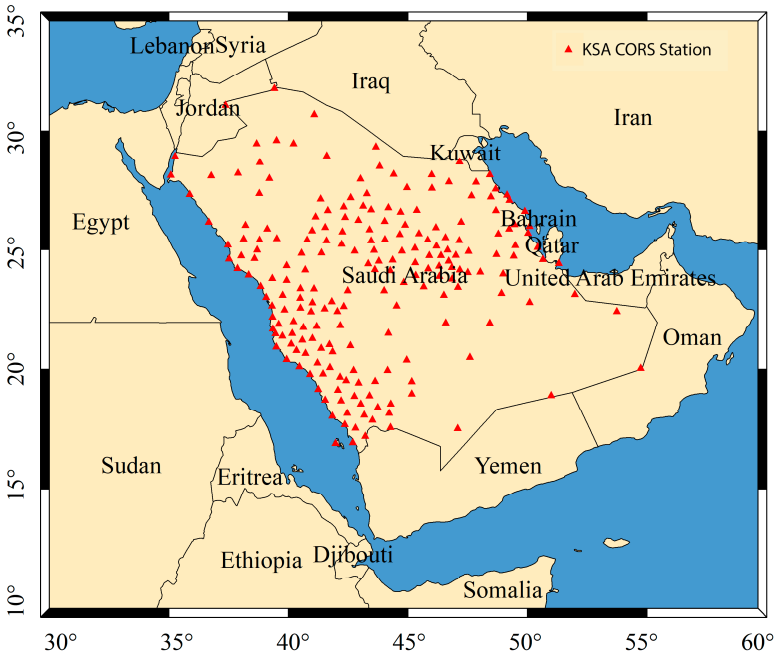


**Figure 2.** KSA-CORS network.

## 3. Field Test and Methodology

To examine the performance of NRTK in hydrographic surveying, a hydrographic surveying test was carried out at Sharm Obhur, where the Faculty of Maritime Studies (FMS) is located, using the KAU-Hydrography 2 vessel on 30 April 2022. KAU-Hydrography 2 is a hydrographic vessel owned by the marine vessels center, King Abdulaziz University, Figure 3. It is equipped with a Teledyne RESON SeaBat T50-P multibeam echosounder and dual-frequency Trimble BD982 GNSS receivers. Valeport's sound velocity profiler (SVP) was used to measure velocity, temperature, and pressure through water layers. Applanix POS MV was used to blend GNSS data with angular rate and acceleration data from LN-200 state-of-the art IMU and heading from the GNSS Azimuth Measurement System (GAMS) to obtain a robust and accurate position and orientation solution.

NRTK corrections were streamed in real time from the KSA-CORS NTRIP server to obtain the NRTK real-time solution. A Trimble SPS855 GNSS receiver was used to establish the base station on the rooftop of the FMS main building to simultaneously collect GNSS data. The observations from the GNSS base station and primary GNSS rover receiver were integrated with INS navigation data in a tightly coupled scheme using the Klaman filter using the Applanix POSPac MMS IN-Fusion Single Base processing option to generate the

smoothed best estimate of trajectory (SBET) file, Figure 4. Such generated SBET was used as the reference solution, which the NRTK solution was compared with. Figure 5 shows the field test trajectory and the location of the base station. The distance between the base station and the vessel was maintained within 1.0 km during the survey session to have the best reference solution.


**Figure 3.** KAU-Hydrography 2 vessel.

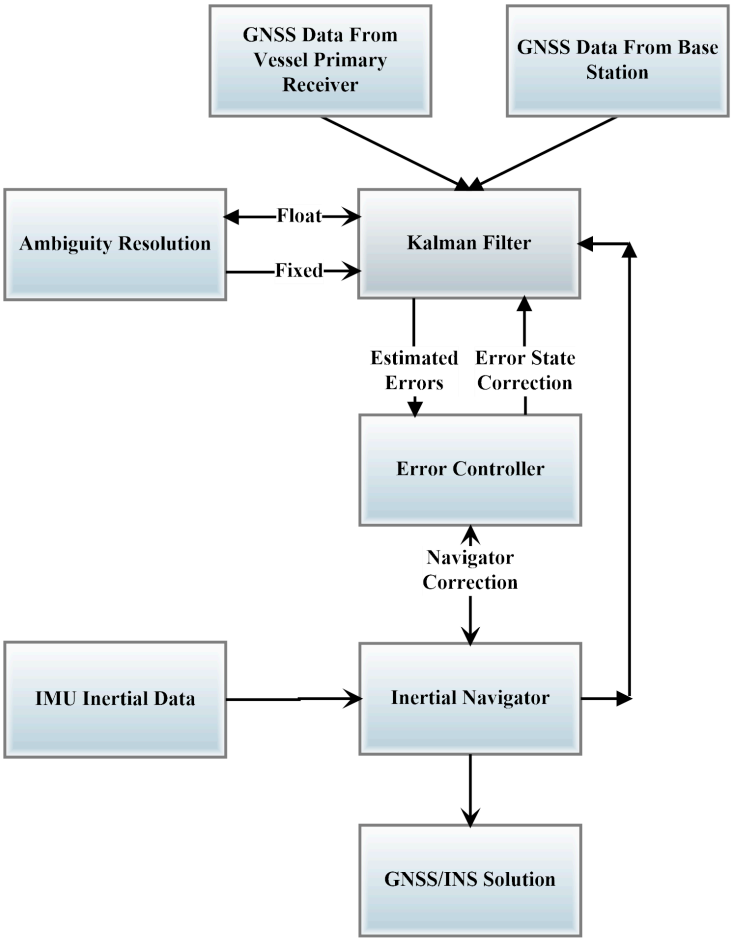


**Figure 4.** Tightly coupled GNSS/INS integration.

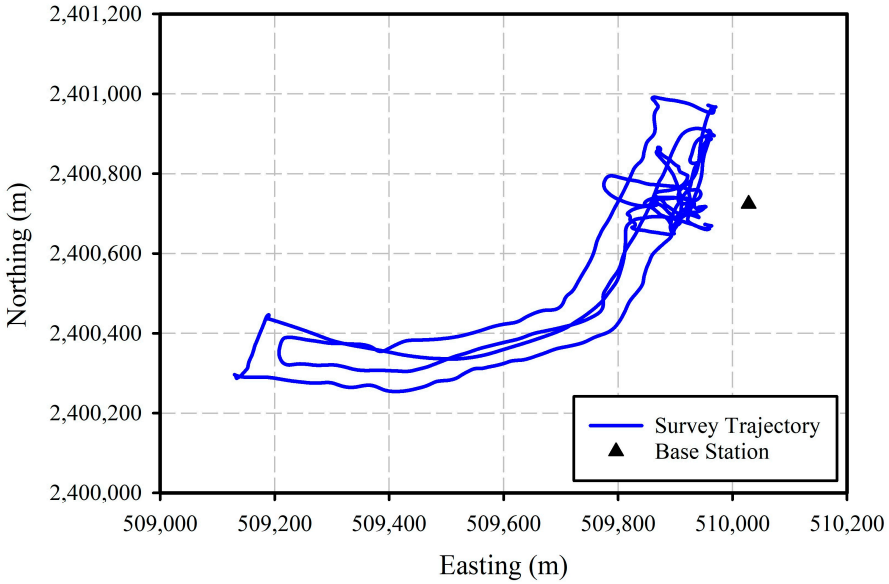


**Figure 5.** Field test trajectory.

NRTK corrections are streamed in real time from the KSA-CORS NTRIP server to obtain the NRTK real-time solution. A Trimble SPS855 GNSS receiver was used to establish the base station.

## 4. Results and Discussion

The vessel trajectory generated in real time using the KSA-CORS NRTK solution is compared with the reference post-processed kinematic (PPK) solution. Figure 6 shows easting, northing, up, and 3-D NRTK errors. Figure 7, on the other hand, shows the two-dimensional (2D) and one-dimensional (up) NRTK errors.

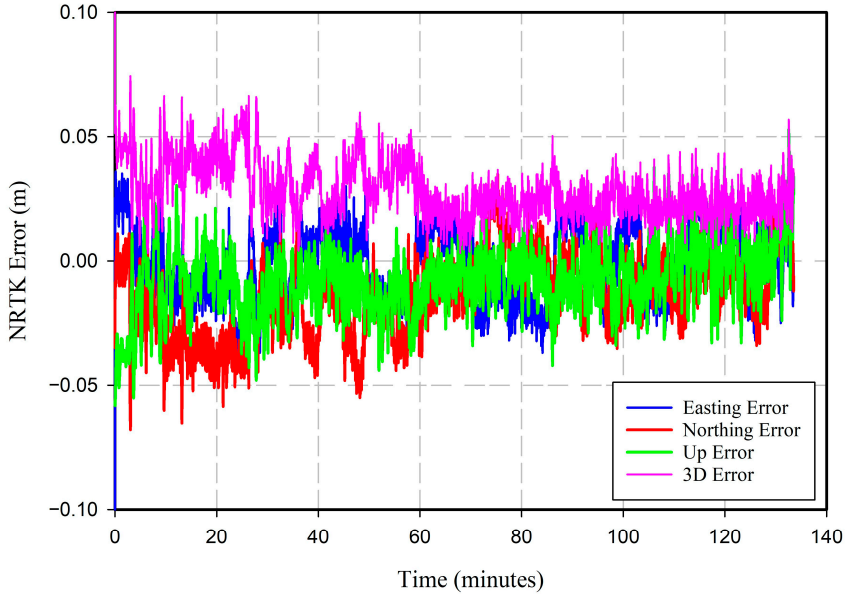


**Figure 6.** NRTK positioning errors.

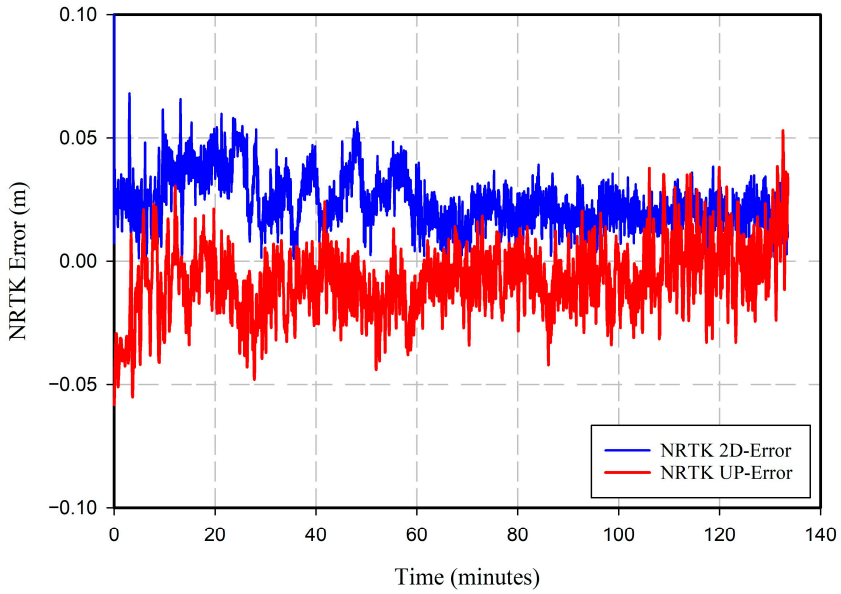


**Figure 7.** NRTK 2-D and up positioning errors.

To determine whether NRTK satisfies the IHO minimum standards of hydrographic surveys, both the total horizontal uncertainty (THU) and the total vertical uncertainty (TVU) were computed at a 95% confidence level, as follows [42]:

$$THU_{95\%}^{2D} = 2.44\sqrt{\frac{\sum_{i=1}^{n}\left[\left(\hat{N}_{NRTK} - \hat{N}_{PPK}\right)_i^2 + \left(\hat{E}_{NRTK} - \hat{E}_{PPK}\right)_i^2\right]}{n}} \quad (5)$$

$$TVU_{95\%}^{1D} = 1.96\sqrt{\frac{\sum_{i=1}^{n}\left(\hat{U}_{NRTK} - \hat{U}_{PPK}\right)_i^2}{n}} \quad (6)$$

where $THU_{95\%}^{2D}$ represents the total 2D horizontal uncertainty of northing and easting position error at a 95% confidence level; $\hat{N}_{NRTK}$, $\hat{E}_{NRTK}$, and $\hat{U}_{NRTK}$ are the northing, easting, and up coordinates of the NRTK solution, respectively; $\hat{N}_{PPK}$, $\hat{E}_{PPK}$, and $\hat{U}_{PPK}$ are the northing, easting, and up coordinates of the PPK solution (the reference solution); $n$ is the total number of epochs; and $TVU_{95\%}^{1D}$ represents the total 1D vertical uncertainty of the up component at a 95% confidence level.

The IHO minimum bathymetry standards for the safety of navigation hydrographic surveys at a 95% confidence level, on the other hand, can be computed as follows [43]:

$$THU = const. + \%\text{ of depth} \quad (7)$$

$$TVU = \pm\sqrt{a^2 + (b \times d)^2} \quad (8)$$

where $a$ represents the portion of the uncertainty that does not vary with depth; $b$ is a coefficient that represents the portion of the uncertainty that varies with depth; and $d$ is the depth. The depth values used in Tables 3 and 4 are 40 m for exclusive and special survey orders and 100 m for other survey orders.

Our results showed that $THU_{95\%}^{2D}$ and $TVU_{95\%}^{1D}$ are 6.38 cm and 3.10 cm, respectively. Comparing the estimated values with the IHO minimum bathymetry standards for the safety of navigation hydrographic surveys at a 95% confidence level (Tables 3 and 4) shows that the NRTK solution successfully meets the minimum standards of IHO requirements of hydrographic surveys. To further investigate the impact of the NRTK positioning technique on the generated seabed surface, Caris HIPS and SIPS 11.00 software was used to process

the multibeam data and generate two gridded surfaces at a resolution of 0.50 m. Figure 8 shows the reference surface, which represents the bathymetry of the survey area estimated using the PPK technique. The main difference between NRTK and PPK surfaces is the source of the navigation data used in Caris HIPS and SIPS processing. Caris HIPS and SIPS software is used to compare the NRTK-based and PPK-based surfaces. Figure 9 shows the differences between the NRTK surface and the reference (PPK) surface.

**Table 3.** International Hydrography Organization (IHO) minimum standards for hydrographic surveys (THU) [43].

| Survey Order | Exclusive | Special | 1a | 1b | 2 |
|---|---|---|---|---|---|
| Constant [m] | 1 | 2 | 5 | 5 | 20 |
| Variable [% of depth] | 0 | 0 | 5 | 5 | 10 |
| THU (m) | 1 | 2 | 10 | 10 | 30 |

**Table 4.** IHO minimum standards for hydrographic surveys (TVU) [43].

| Survey Order | Exclusive | Special | 1a | 1b | 2 |
|---|---|---|---|---|---|
| Constant (a) [m] | 0.15 | 0.25 | 0.50 | 0.50 | 1.00 |
| Variable (b) [% of depth] | 0.75 | 0.75 | 1.30 | 1.30 | 2.30 |
| TVU (m) | 0.34 | 0.39 | 1.39 | 1.39 | 2.51 |

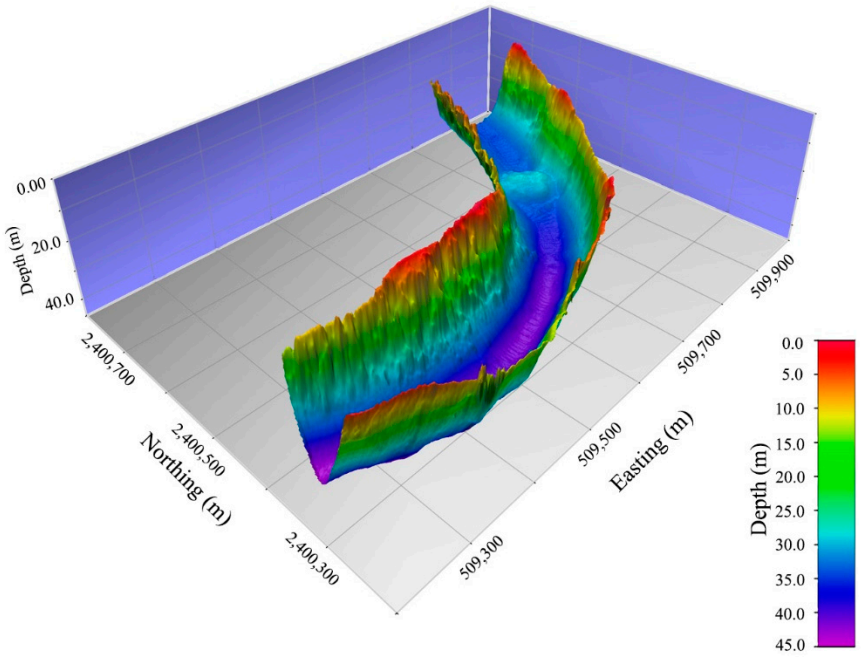


**Figure 8.** Bathymetry of the survey area.

Figure 9 shows that the differences between the bathymetry obtained using the NRTK technique and the bathymetry derived from the PPK exist at the outer beams close to the channel edges. Based on the navigation data source, any change in the horizontal position will produce large changes in the depth, especially at steep edges of the navigation channel. The number of points at which maximum and minimum differences occur are very few. However, it is clear from Figure 9 that most of the surface differences lie within 2 mm. Table 5 summarizes the statistical analysis of the PPK-NRTK bathymetry difference.

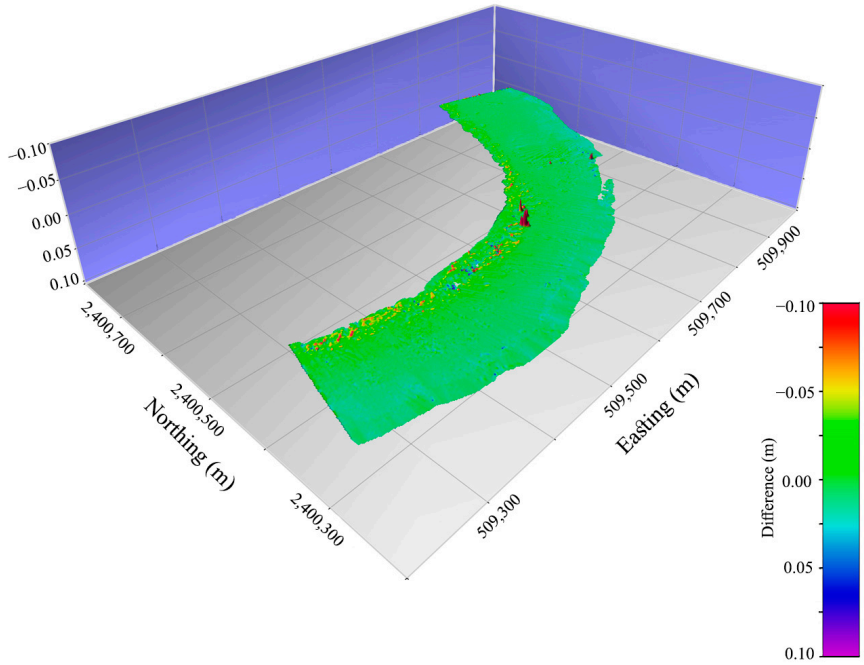


**Figure 9.** Differences between PPK and NRTK bathymetry.

**Table 5.** Statistical analysis of bathymetry differences.

| | **PPK-NRTK** |
|---|---|
| Minimum (m) | −2.85 |
| Maximum (m) | 1.01 |
| Mean (cm) | −0.19 |
| Standard Deviation (cm) | 2.40 |
| Total Count | 1,866,378 |

Statistical analysis of the PPK-NRTK bathymetry differences, Table 5, shows that the mean difference is −0.19 cm, and the corresponding standard deviation is 2.4 cm, which means using real-time corrections from KSA-CORS can achieve comparable results with the PPK technique without the need of reference station in the survey area. Therefore, having a national network of CORS in the country will have a great economic impact on project development, including hydrographic surveying.

## 5. Conclusions

This paper evaluated the performance of the NRTK technique compared with the traditional RTK technique in hydrographic surveys and then investigated if the NRTK technique meets the minimum standards of IHO for hydrographic surveys. A hydrographic survey session was conducted at Sharm Obhur in front of the Faculty of Maritime Studies, King Abdulaziz University using the KAU-Hydrography 2 vessel. NRTK corrections were streamed in real time from the KSA-CORS NTRIP server, and base station GNSS data were collected at the same time using a Trimble SPS855 GNSS receiver. Multibeam records were collected using a Teledyne RESON SeaBat T50-P multibeam echosounder in addition to Valeport's sound velocity profiler records and Applanix POSMV data. It is shown that the $THU^{2D}_{95\%}$ and $TVU^{1D}_{95\%}$ of the NRTK solution are 6.38 cm and 3.10 cm, respectively. Statistical analysis of the differences between the seabed surface generated using the NRTK solution and the seabed surface generated using the PPK technique showed an average of −0.19 cm and a standard deviation of 2.4 cm. From these results, we can conclude that the

KSA-CORS NRTK solution successfully meets IHO minimum bathymetry standards for the safety of navigation hydrographic surveys at a 95% confidence level for all orders of hydrographic surveys.

In future research, there are plans to use the local CORS in Jeddah city to obtain the same NRTK corrections. This network is smaller than the KSA-CORS, and server performance will then be investigated by simultaneously receiving correction from different locations in the city with different setups. Another point that should be further investigated is how far users can receive valid corrections in the open sea away from the network.

**Funding:** This research was funded by the Deanship of Scientific Research (DSR) at King Abdulaziz University (KAU), Jeddah, under grant number G: 639-980-1443.

**Institutional Review Board Statement:** Not Applicable.

**Informed Consent Statement:** Not Applicable.

**Data Availability Statement:** Data are contained within the article.

**Acknowledgments:** The author acknowledges and thanks DSR's technical and financial support. The author acknowledges the General Authority for Survey and Geospatial Information (GASGI) for providing access to KSA-CORS data and products.

**Conflicts of Interest:** The author declares no conflicts of interest.

## References

1. Elsobeiey, M.; El-Rabbany, A. GPS precise point positioning: Some recent developments. In Proceedings of the the First International Geomatics Symposium in Saudi Arabia in Collaboration with the INSA-Strasbourg and the University of Florida, Jeddah, Saudi Arabia, 10–13 May 2011.
2. El-Rabbany, A. An Autonomous GPS Carrier-Phased-Based System for Precision Navigation. In Proceedings of the 2006 IEEE Intelligent Transportation Systems Conference, Toronto, ON, Canada, 17–20 September 2006; pp. 783–787.
3. Cina, A.; Dabove, P.; Manzino, A.M.; Piras, M. Network real time kinematic (NRTK) positioning–description, architectures and performances. In *Satellite Positioning-Methods, Models and Applications*; InTech: Rijeka, Croatia, 2015; pp. 23–45.
4. Hofmann-Wellenhof, B.; Lichtenegger, H.; Wasle, E. *GNSS Global Navigation Satellite Systems. GPS, Glonass, Galileo & More*; Springer Wien: New York, NY, USA, 2008; p. xxix, 516p.
5. Vollath, U.; Buecherl, A.; Landau, H.; Pagels, C.; Wagner, B. Multi-base RTK positioning using virtual reference stations. In Proceedings of the 13th International Technical Meeting of the Satellite Division of The Institute of Navigation (ION GPS 2000), Salt Lake City, UT, USA, 19–22 September 2000; pp. 123–131.
6. Kjørsvik, N. Assessing the multi-base station GPS solutions. In Proceedings of the FIG XXII International Congress, Washington, DC, USA, 19–26 April 2002.
7. Landau, H.; Vollath, U.; Chen, X. Virtual reference stations versus broadcast solutions in network RTK–advantages and limitations. In Proceedings of the GNSS, Graz, Austria, 22–24 April 2003; pp. 22–25.
8. Gordini, C.; Abbondanzab, C.; Barbarellab, M. GNSS network real time positioning: Testing procedure to evaluate the accuracy of a geodetic moving antenna. In *International Archives of the Photogrammetry, Remote Sensing and Spatial Information Sciences—ISPRS Archives, 36 (5C55)*; ISPRS: Hannover, Germany, 2015.
9. Aponte, J.; Meng, X.; Hill, C.; Moore, T.; Burbidge, M.; Dodson, A. Quality assessment of a network-based RTK GPS service in the UK. *J. Appl. Geod.* **2009**, *3*, 25–34. [CrossRef]
10. Dardanelli, G.; Lo Brutto, M.; Franco, V. Accuracy and reliability in GNSS NRTK. In Proceedings of the European Navigation Conference—Global Navigation Satellite Systems, Naples, Italy, 3–6 May 2009.
11. Jamil, H.; Mohamed, A.; Chang, D. The Malaysia real-time kinematic GNSS network (MyRTKnet) in 2010 and beyond. In Proceedings of the FIG Congress 2010, Sydney, Australia, 11–16 April 2010; pp. 11–16.
12. Stateczny, A.; Specht, C.; Specht, M.; Brčić, D.; Jugović, A.; Widźgowski, S.; Wiśniewska, M.; Lewicka, O. Study on the Positioning Accuracy of GNSS/INS Systems Supported by DGPS and RTK Receivers for Hydrographic Surveys. *Energies* **2021**, *14*, 7413. [CrossRef]
13. Ouassou, M.; Natvig, B.; Jensen, A.B.O.; Gåsemyr, J.I. Reliability Analysis of Network Real-Time Kinematic. *J. Electr. Comput. Eng.* **2018**, *2018*, 8260479. [CrossRef]

14. Ouassou, M.; Jensen, A.B.O. Network real-time kinematic data screening by means of multivariate statistical analysis. *SN Appl. Sci.* **2019**, *1*, 512. [CrossRef]
15. El-Diasty, M. A real-time KSACORS-based NRTK GNSS positioning system for Saudi coastal navigation. *Aust. J. Marit. Ocean. Aff.* **2020**, *12*, 95–107. [CrossRef]
16. Zhang, M.; Lü, J.; Bai, Z.; Liu, H.; Fan, C. Improving the initialization speed for long-range NRTK in network solution mode. *Sci. China Technol. Sci.* **2020**, *63*, 866–873. [CrossRef]
17. Gökdaş, Ö.; Özlüdemir, M.T. A Variance Model in NRTK-Based Geodetic Positioning as a Function of Baseline Length. *Geosciences* **2020**, *10*, 262. [CrossRef]
18. De Andrade Neto, W.P.; Paz, I.d.S.R.; Oliveira, R.A.A.C.e.; De Paulo, M.C.M. Comparison of the vertical accuracy of satellite-based correction service and the PPK GNSS method for obtaining sensor positions on a multibeam bathymetric survey. *Sci. Rep.* **2024**, *14*, 11104. [CrossRef] [PubMed]
19. Santana, F.; Krueger, C.; Baluta, É.; Santana, T.; De Moraes Vestena, K. Evaluation of precise point positioning and post-processing kinematic methods for tide measurement in hydrographic surveys. *Bol. Ciências Geodésicas* **2024**, *30*, e2024008. [CrossRef]
20. Elsheikh, M.; Iqbal, U.; Noureldin, A.; Korenberg, M. The Implementation of Precise Point Positioning (PPP): A Comprehensive Review. *Sensors* **2023**, *23*, 8874. [CrossRef] [PubMed]
21. Elsobeiey, M. Precise Point Positioning using Triple-Frequency GPS Measurements. *J. Navig.* **2015**, *68*, 480–492. [CrossRef]
22. Geng, J.; Wen, Q.; Zhang, Q.; Li, G.; Zhang, K. GNSS observable-specific phase biases for all-frequency PPP ambiguity resolution. *J. Geod.* **2022**, *96*, 11. [CrossRef]
23. Collins, P.; Bisnath, S.; Lahaye, F.; Heroux, P. Undifferenced GPS Ambiguity Resolution Using the Decoupled Clock Model and Ambiguity Datum Fixing. *Navigation J. Inst. Navig.* **2010**, *57*, 123–135. [CrossRef]
24. Elsobeiey, M.; El-Rabbany, A. Efficient Between-Satellite Single-Difference Precise Point Positioning Model. *J. Surv. Eng.* **2014**, *140*, 04014007. [CrossRef]
25. Hou, Z.; Zhou, F. Assessing the Performance of Precise Point Positioning (PPP) with the Fully Serviceable Multi-GNSS Constellations: GPS, BDS-3, and Galileo. *Remote Sens.* **2023**, *15*, 807. [CrossRef]
26. Zheng, Y.; Zheng, F.; Yang, C.; Nie, G.; Li, S. Analyses of GLONASS and GPS+GLONASS Precise Positioning Performance in Different Latitude Regions. *Remote Sens.* **2022**, *14*, 4640. [CrossRef]
27. Wu, M.; Wang, L.; Xie, W.; Yue, F.; Cui, B. Performance Evaluation and Application Field Analysis of Precise Point Positioning Based on Different Real-Time Augmentation Information. *Remote Sens.* **2024**, *16*, 1349. [CrossRef]
28. Elsobeiey, M.; Al-Harbi, S. Performance of real-time Precise Point Positioning using IGS real-time service. *GPS Solut.* **2016**, *20*, 565–571. [CrossRef]
29. El-Diasty, M.; Elsobeiey, M. Precise Point Positioning Technique with IGS Real-Time Service (RTS) for Maritime Applications. *Positioning* **2015**, *6*, 71–80. [CrossRef]
30. Specht, M. Testing and Analysis of Selected Navigation Parameters of the GNSS/INS System for USV Path Localization during Inland Hydrographic Surveys. *Sensors* **2024**, *24*, 2418. [CrossRef] [PubMed]
31. Huang, Z.; Jin, S.; Su, K.; Tang, X. Multi-GNSS Precise Point Positioning with UWB Tightly Coupled Integration. *Sensors* **2022**, *22*, 2232. [CrossRef] [PubMed]
32. Li, S.; Li, X.; Wang, H.; Zhou, Y.; Shen, Z. Multi-GNSS PPP/INS/Vision/LiDAR tightly integrated system for precise navigation in urban environments. *Inf. Fusion* **2023**, *90*, 218–232. [CrossRef]
33. Koivula, H.; Kuokkanen, J.; Marila, S.; Lahtinen, S.; Mattila, T. Assessment of sparse GNSS network for network RTK. *J. Geod. Sci.* **2018**, *8*, 136–144. [CrossRef]
34. Kleusberg, A.; Teunissen, P.J.G. *GPS for Geodesy*, 2nd, completely rev. and extended ed.; Springer: Berlin/Heidelberg, Germany, 1998; p. xiv, 650p.
35. Euler, H.J.; Keenan, R.; Zebhauser, B.; Wübbena, G. Study of a Simplified Approach in Utilizing Information from Permanent Reference Station Arrays. In Proceedings of the 14th International Technical Meeting of the Satellite Division of The Institute of Navigation ION GPS, Salt Lake City, UT, USA, 11–14 September 2001; pp. 379–391.
36. Brown, N.; Geisler, I.; Troyer, L. RTK Rover Performance using the Master-Auxiliary Concept. *J. Glob. Position. Syst.* **2006**, *5*, 135–144. [CrossRef]
37. Janssen, V. A comparison of the VRS and MAC principles for network RTK. In Proceedings of the IGNSS 2009 Symposium, Surfers Paradise, Australia, 1–3 December 2009.
38. Brown, N.; Keenan, R.; Richter, B.; Troyer, L. Advances in Ambiguity Resolution for RTK Applications Using the New RTCM V3.0 Master-Auxiliary Messages. In Proceedings of the 18th International Technical Meeting of the Satellite Division of The Institute of Navigation (ION GNSS 2005), Long Beach, CA, USA, 13–16 September 2005.
39. GASGI. *Getting Started with KSA-CORS Network*; General Directorate of Geodesy: Riyadh, Saudi Arabia, 2020; Volume 1, p. 15.
40. GASGI. *Saudi Arabia National Spatial Reference System Implementation Guidelines*; GEOSA: Riyadh, Saudi Arabia, 2021.
41. GASGI. *Technical Summary for Saudi Arabia National Spatial Reference System (SANSRS)*; GEOSA: Riyadh, Saudi Arabia, 2021.

42. Elsobeiey, M.E. Accuracy Assessment of Satellite-Based Correction Service and Virtual GNSS Reference Station for Hydrographic Surveying. *J. Mar. Sci. Eng.* **2020**, *8*, 542. [CrossRef]
43. IHO. *International Hydrographic Organization Standards for Hydrographic Surveys*, 6.1.0. ed.; Special Publication No. 44; International Hydrographic Bureau: Monaco, 2022; Available online: https://iho.int/uploads/user/pubs/standards/s-44/S-44_Edition_6.1.0.pdf (accessed on 15 October 2024).